THE JOURNAL OF PHYSICAL CHEMISTRY C

Article

Structure Sensitivity in Adsorption and Decomposition of NO on Ir

Wenhua Chen, Theodore E. Madey, Alan L. Stottlemyer, Jingguang G. Chen, Payam Kaghazchi, and Timo Jacob

J. Phys. Chem. C, **2008**, 112 (48), 19113-19120 • DOI: 10.1021/jp808143p • Publication Date (Web): 11 November 2008

Structure Sensitivity in Adsorption and Decomposition of NO on Ir

Wenhua Chen* and Theodore E. Madey

Department of Physics and Astronomy, and Laboratory for Surface Modification, Rutgers, The State University of New Jersey, Piscataway, New Jersey 08854

Alan L. Stottlemyer and Jingguang G. Chen

Department of Chemical Engineering, University of Delaware, Newark, Delaware 19716;

Payam Kaghazchi

Fritz-Haber-Institut der Max-Planck-Gesellschaft, Faradayweg 4-6, D-14195 Berlin, Germany

Timo Jacob

Fritz-Haber-Institut der Max-Planck-Gesellschaft, Faradayweg 4-6, D-14195 Berlin, Germany and Theoretische Elektrochemie, Universität Ulm, Albert-Einstein-Allee 47, D-89 069 Ulm, Germany

Received: September 12, 2008; Revised Manuscript Received: October 14, 2008

The adsorption and decomposition of NO on planar Ir(210) and nanofaceted Ir(210) with tunable facet sizes (5−14 nm) have been studied by means of temperature programmed desorption (TPD), high-resolution electron energy loss spectroscopy (HREELS), and density functional theory (DFT). Evidence has been found for structure sensitivity in adsorption sites and thermal decomposition of NO on planar Ir(210) versus those on faceted Ir(210). Both planar and faceted Ir(210) surfaces are very active for NO decomposition with high selectivity to N_2. Heating NO-saturated *planar* Ir(210) leads to desorption of large amounts of N_2 and small amounts of NO together with traces of N_2O. Annealing NO-saturated *faceted* Ir(210) also produces large amounts of N_2 and small amounts of NO without the formation of N_2O. Adsorption of NO at 300 K on both surfaces is predominantly molecular. On planar Ir(210) NO adsorbs on atop sites for the entire NO coverage range. On faceted Ir(210) that contains (110) and {311} faces, NO adsorbs on bridge and atop sites at low NO coverage while only on atop sites at high NO coverage. No evidence has been found for size effects in the thermal decomposition of NO over faceted Ir(210) for average facet size ranging from 5 to 14 nm.

1. Introduction

Catalytic conversion of nitric oxide (NO) to nitrogen (N_2) has been a topic of significant interest because it is a key step in reducing air pollution from automotive exhaust gases. Both catalytic reduction and decomposition of NO have been intensely studied.[1,2] The selective catalytic reduction (SCR) of NO by hydrocarbons is believed to be the most promising way to eliminate NO.[1] Recent reports show that among noble metals for the SCR of NO by hydrocarbons, platinum- and iridium-based catalysts are the most active ones[3] and Ir is more active and selective than Pt at higher temperatures.[4] Notably, Pt is a catalyst component in the current commercial three-way catalysts. However, the SCR of NO by hydrocarbons can lead to production of secondary pollutants such as oxygenated hydrocarbons, CO, and N_2O. One way to avoid these secondary pollutants except N_2O formation is the decomposition of NO to N_2, which receives increasing interest and is likely the most attractive solution in pollution control.[1] Extensive studies of NO decomposition have been carried out over various supported and unsupported metal catalysts, and it has been shown that both the support and the metallic particle size influence the catalytic activity toward the decomposition of NO.[1,2]

In this work, an Ir(210) crystal is used to prepare in situ two structurally different Ir surfaces of clean *planar* Ir(210) and clean *faceted* Ir(210) for investigating the decomposition of NO, free of any support material. The atomically rough Ir(210) surface remains planar when exposed to oxygen at 300 K. However, when O-covered planar Ir(210) is annealed to temperatures ≥ 600 K, nanoscale three-sided pyramidal facets grow and cover the surface (Figure 1).[5,6] Note that facet orientation is essentially independent of oxygen coverage, which is in contrast to O-induced faceting of Re($12\bar{3}1$) and Re($11\bar{2}1$) as well as O-induced faceting of Ru($11\bar{2}0$) (NO_2 is used in the experiment), where a clear coverage-dependent morphological evolution of the facets is observed.[7−10] After facet formation, the surface oxygen can be completely removed to prepare clean faceted Ir(210) using H_2 at 400 K.[6,11,12] By changing the annealing temperature for the formation of O-covered faceted Ir(210), it is possible to control the average pyramid size from ∼5 nm to ∼14 nm.[6,12] Thus, both clean planar Ir(210) and clean nanofaceted Ir(210) with tunable facet sizes on the nanometer scale can be prepared, which enables investigation of structure sensitivity and size effects in the decomposition of NO on unsupported Ir with well-defined surface structure and controlled size. Here, we provide experimental evidence that model Ir surfaces exhibit unusually higher reactivity and selectivity to N_2 in direct decomposition of NO, compared to model Pt surfaces. In addition, we show evidence for structure sensitivity

* Author to whom correspondence should be addressed. E-mail: wchen@physics.rutgers.edu.

10.1021/jp808143p CCC: $40.75
Published on Web 11/11/2008

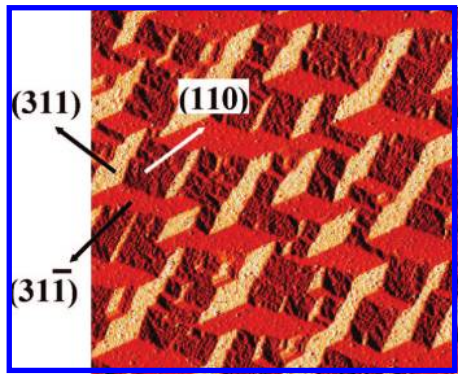

Figure 1. STM image (100 nm × 100 nm) from oxygen-covered faceted Ir(210) showing the morphology of three-sided pyramidal facets. Reprinted with permission from ref 6. Copyright (2005) American Chemical Society.

in adsorption sites and thermal decomposition of NO on planar Ir(210) versus faceted Ir(210). The combination of temperature programmed desorption (TPD), high resolution electron energy loss spectroscopy (HREELS), and density functional theory (DFT) employed in this work has proven to be very powerful for studying the chemistry of NO on metal surfaces.

This paper is organized as follows. After a description of the experimental and theoretical procedures, the N_2, NO, and N_2O TPD data from NO on planar Ir(210) in the absence and presence of preadsorbed CO as well as data from NO on faceted Ir(210) are presented. This is followed by surface characterization of NO-covered planar and faceted Ir(210) using HREELS and DFT calculations of binding sites and vibrational frequencies for NO on the Ir surfaces. The discussion emphasizes the reactivity and selectivity to N_2 of planar and faceted Ir(210) for NO decomposition and evidence for structure sensitivity in adsorption sites and thermal decomposition of NO on planar Ir(210) versus faceted Ir(210). The comparison of reactivity and selectivity to N_2 of planar and faceted Ir(210) with other platinum group metals in NO decomposition is also discussed.

2. Experimental and Computational Procedures

TPD experiments were performed at Rutgers University in an ultrahigh vacuum (UHV) chamber equipped with Auger electron spectroscopy (AES), low-energy electron diffraction (LEED), and a quadrupole mass spectrometer (QMS).[11] All TPD spectra were measured at a sample heating rate of ~5 K/s. HREELS measurements were made at University of Delaware in a previously described UHV system,[11] which contained AES, LEED, QMS, and HREELS. The HREELS spectrometer (LK 3000) was operated at electron energy of 6.0 eV with a typical resolution between 40 and 60 cm^{-1}. All HREEL spectra were recorded in the specular direction at an angle of 60° with the sample held at 130−150 K.

The same Ir(210) crystal was used in both laboratories. The sample mounting and cleaning procedures at Rutgers were different from those at Delaware. At Rutgers, the sample was spot-welded to two Re ribbon leads that are attached to the Mo rods for support and resistive heating. The sample could be heated to 1300 K by resistive heating, i.e., passing DC current through the sample, or 2000 K by e-beam heating from a W filament behind the Ir(210) crystal. The sample temperature was measured using a W-5%Re/W-26%Re thermocouple that was spot-welded to the back of the sample. At Delaware, the sample was spot-welded to two Ta wires for support and resistive heating and a type K thermocouple was used to monitor the sample temperature. The sample was cleaned by Ne^+ sputtering and annealing in O_2, H_2, and UHV as described below.

At Rutgers, procedures to prepare clean planar Ir(210) and clean faceted Ir(210) have been described previously.[6,11,12] In short, clean planar Ir(210) was prepared by cycles of flashing the sample to 1700 K in O_2 (5×10^{-8} Torr) to remove surface carbon contamination followed by flashing to 1700 K in UHV to remove surface oxygen. Clean faceted Ir(210) was generated by annealing clean planar Ir(210) in O_2 (5×10^{-8} Torr) at 600−1700 K and subsequent cooling in O_2 to 300 K to form O-covered faceted Ir(210), which was followed by a reaction with H_2 at 400 K to remove surface oxygen. By changing the annealing temperature from 600 K to 1700 K for the formation of O-covered faceted Ir(210) we can control the average facet size from 5 nm to 14 nm.[6,12]

At Delaware, the clean planar Ir(210) surface was generated by cycles of Ne^+ sputtering (3 kV and 8−10 μA) and annealing at 700 K in O_2 (5×10^{-8} Torr) to remove surface carbon contamination followed by annealing at 400 K in H_2 (1×10^{-8} Torr) and heating to 700 K in UHV to remove surface oxygen and relax faceted Ir(210) to planar Ir(210). The clean faceted Ir(210) surface was generated by annealing clean planar Ir(210) in O_2(5×10^{-8} Torr) at 600 K for 2 min and subsequent cooling in O_2 to 300 K to form O-covered faceted Ir(210), which was followed by a reaction with H_2 at 400 K to remove surface oxygen. This produced clean faceted Ir(210) surface with an average facet size of 5 nm.[6,12]

In all experiments, ^{15}NO was used to distinguish $^{15}N_2$ from CO and $^{15}N_2O$ from CO_2 in TPD. Research purity ^{15}NO, H_2, and O_2 were used without further purification, and the gases were dosed onto the Ir surfaces at 300 K by backfilling the chamber. All exposures are reported in Langmuir (1 L = 10^{-6} Torr·s = 1.3×10^{-4} Pa·s) and uncorrected for ion gauge sensitivity. The surface cleanliness is checked using AES and TPD while surface structure is monitored by LEED. The planar Ir(210) surface is an atomically rough surface with four layers exposed, which contains coordination sites C_6, C_9, C_{11}, and C_{12} where the subscript denotes the number of nearest-neighbor atoms.[11] Faceted Ir(210) consists of three-sided nanoscale pyramids exposing two different kinds of facets (one (110) face and two {311} faces on each pyramid) (see Figure 1).[5,6]

The binding energies and vibrational frequencies of NO on Ir(210), Ir(311), and Ir(110) were calculated by DFT using the CASTEP code.[13] Throughout the calculations, optimized ultrasoft pseudopotentials[14] and the generalized gradient approximation (GGA) exchange-correlation functional proposed by Perdew, Burke, and Ernzerhof (PBE)[15] were used. The Ir(210), Ir(311), and Ir(110) surfaces were represented by 16-layer, 11-layer, and 12-layer slabs with ~12 A vacuum, respectively. The bottom three layers for Ir(210) and Ir(311) and the bottom four layers for Ir(110) were fixed at the calculated bulk structures and the geometries of the remaining layers and the adsorbates were allowed to fully optimize. For all NO-adsorbed systems, a cutoff energy of 340 eV was employed and the Brilouin zones of the (1 × 1) unit cell of Ir(210), Ir(311), and Ir(110) were sampled with 10 × 8, 14 × 8, and 14 × 10 Monkhorst-Pack k-point meshes,[16] respectively.

3. Results

3.1. TPD Study. The products monitored during TPD for NO adsorbed on planar and faceted Ir(210) surfaces at 300 K are N_2, NO, N_2O, and NO_2. For all NO exposures studied, no desorption of NO_2 is observed and both surfaces are covered by oxygen after TPD. The formation of N_2 is indicative of direct decomposition of NO on planar and faceted Ir(210).

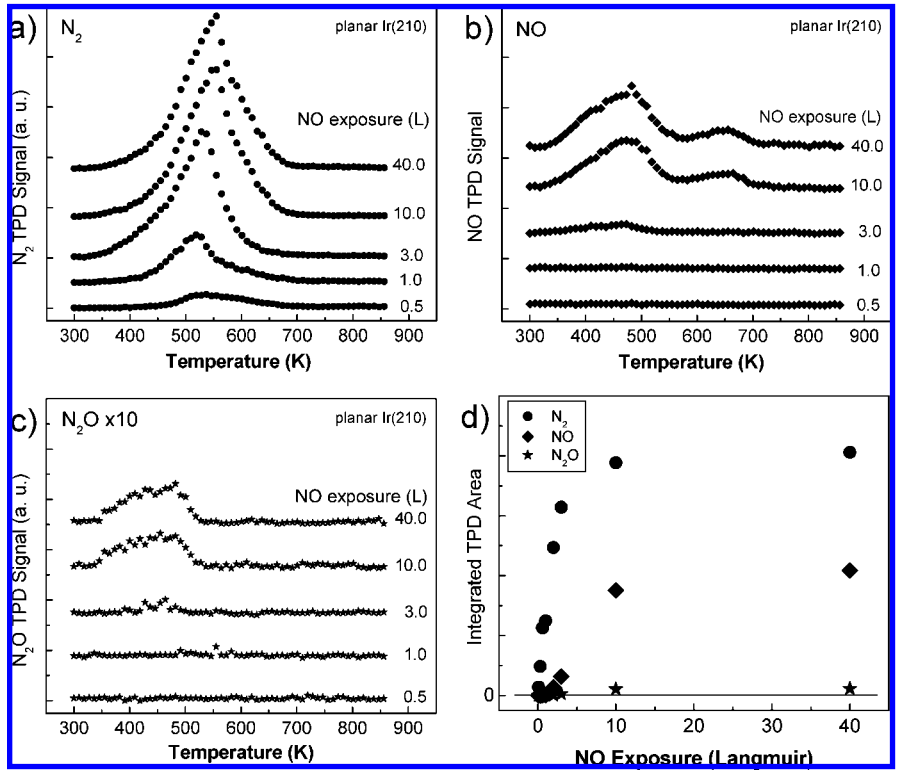

Figure 2. TPD spectra of N_2 (a), NO (b), and N_2O (c) following adsorption of NO on Ir(210) at 300 K. The integrated areas under TPD spectra of N_2, NO, and N_2O from NO on Ir(210) are shown in (d).

3.1.1. NO on Planar Ir(210). Figure 2a−c shows typical TPD spectra of N_2, NO, and N_2O following adsorption of different exposures of NO on Ir(210) at 300 K. At low NO exposure (<3 L), adsorbed NO undergoes complete decomposition to evolve only N_2. As NO exposure increases to ≥3 L, in addition to the dominant N_2 species, a small amount of NO together with traces of N_2O are observed, although no desorption of N_2O is observed from faceted Ir(210) as described in Section 3.1.2. A unique feature in the TPD spectra of N_2 has been observed, i.e., the N_2 peak temperature moves to lower temperatures with increasing NO exposure at low NO exposure (≤1 L of NO) while it shifts to higher temperatures at >1 L of NO exposure. Figure 2d plots the integrated areas under the TPD spectra of N_2, NO, and N_2O as a function of NO exposure. Clearly, the amounts of all three desorbing species increase with NO exposure and reach saturation at 40 L NO.

Figure 3 displays the TPD spectra of N_2 and NO following six consecutive doses of 1 L of NO on Ir(210) at 300 K. No formation of N_2O and NO_2 is observed, and the surface is covered by oxygen after TPD. These measurements are to explore the effects of self-poisoning by the NO decomposition products; no treatment was used to remove residual O deposits between experiments. The successive spectra correspond to 1 L of NO on different surfaces, i.e., clean Ir(210) and Ir(210) covered with different amounts of oxygen deposit. The experiments were performed by dosing 1 L of NO onto clean Ir(210) at 300 K and then measuring the TPD spectra A. After the sample was cooled to 300 K, the surface was exposed again to 1 L of NO, and spectra B were measured. This sequence was repeated for each set of subsequent spectra. In each case, the spectra are different from each other on the six surfaces in their profile and intensity, indicating that each surface has different reactivity for NO decomposition. The surface is still highly active toward decomposition of NO after two cycles of dose/TPD. However, after three cycles of dose/TPD the reactivity

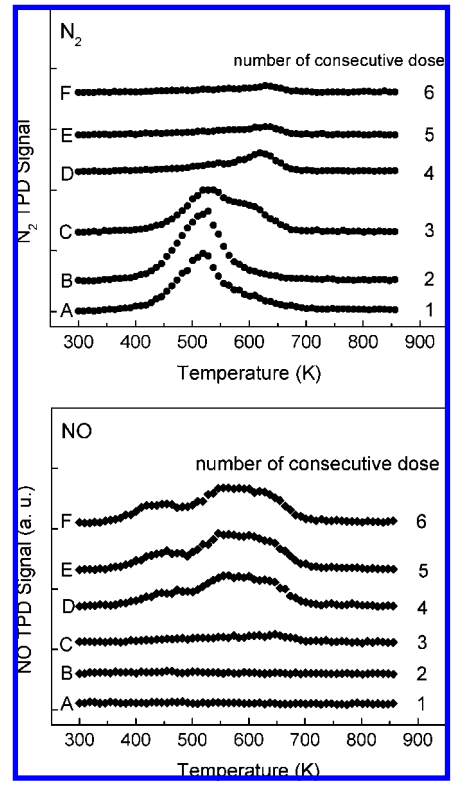

Figure 3. TPD spectra of N_2 and NO following adsorption of consecutive doses of 1 L of NO on Ir(210) at 300 K.

of the surface decreases rapidly in comparison with clean Ir(210), as evidenced by the reduction of N_2 TPD peak area and the growth of NO TPD peak area. This is attributed to a gradual surface site-blocking for NO adsorption as a result of increased oxygen deposit that resulted from the thermal decomposition of NO. Obviously, the continued oxygen ac-

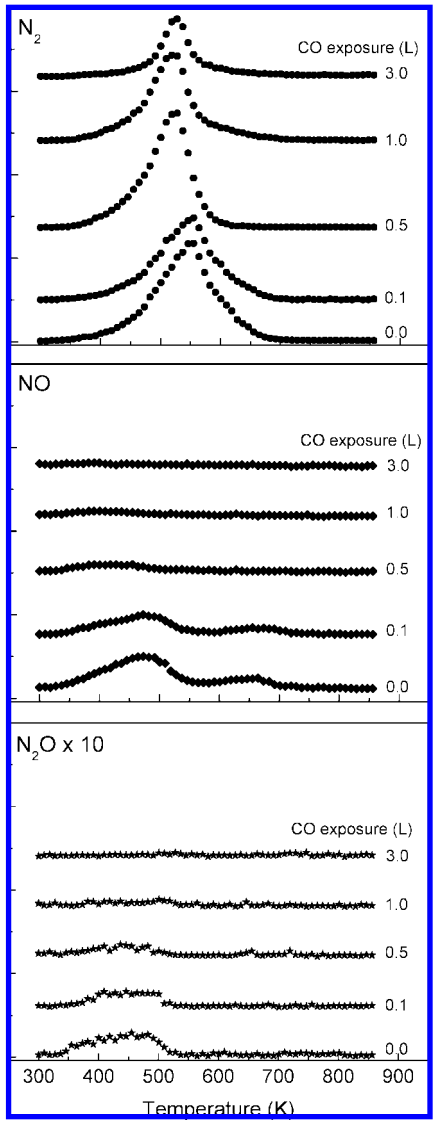

Figure 4. TPD spectra of N_2, NO, and N_2O from adsorption of 10 L of NO on planar Ir(210) predosed with CO at 300 K.

cumulation from NO decomposition eventually deactivates the surface for further decomposition of NO.

We have also investigated the influence of preadsorbed CO on the reduction of NO over Ir(210), as this is of practical importance due to the fact that CO is also present in the exhaust gases. Figure 4 shows TPD spectra of N_2, NO, and N_2O obtained from adsorption of 10 L NO on planar Ir(210), pre-exposed to various amounts of CO at 300 K. No desorption of NO_2 is observed. The spectra of N_2, NO, and N_2O are essentially unchanged with only slight reduction in their intensities when the surface is predosed with 0.1 L of CO. As CO dose increases to 0.5 L, intensities of all three spectra continue to decrease, and the N_2 spectrum changes in profile and shifts to the lower temperature side. Further increasing the CO dose to $\geq$1 L, the intensity of N_2 continues to decrease with increasing CO exposure but no desorption of NO and N_2O is seen. Note that 3 L of CO at 300 K saturates Ir(210) as previously reported.[12] Remarkably, the production of N_2 still occurs without desorption of NO and N_2O even at saturation coverage of preadsorbed CO, indicating that preadsorbed CO does not inhibit conversion of NO to N_2 but improves selectivity to N_2 on Ir(210) from the decomposition of NO.

3.1.2. NO on Faceted Ir(210). When NO is adsorbed on faceted Ir(210) at 300 K and then heated, the products are also dominated by N_2 together with small amount of NO. No formation of N_2O is seen from the faceted surface, in contrast to planar Ir(210) where traces of N_2O are formed as shown in Figure 2. Figure 5 shows the TPD spectra of N_2, NO, and N_2O obtained following adsorption of NO on faceted Ir(210) at 300 K; the TPD spectra from NO on planar Ir(210) with the same doses of NO are also displayed for comparison. For the faceted surfaces of Figure 5, the average facet size is 14 nm. At low NO exposure ($\leq$3 L), N_2 is the only desorption species from the faceted surface, which is indicative of complete decomposition of NO to form N_2. As NO exposure increases to >3 L, a small amount of NO desorbs from the faceted surface in addition to a large amount of N_2 desorption. It is clear from Figure 5 that there are marked differences in reactivity and selectivity to N_2 in the decomposition of NO between planar and faceted Ir(210) surfaces. At 0.5 L NO, planar Ir(210) is more active than faceted Ir(210) as evidenced by a lower onset temperature for N_2 desorption as well as lower temperature for complete desorption of N_2, although NO undergoes complete decomposition on both surfaces. At $\geq$3 L NO, faceted Ir(210) is more active and selective to N_2, as indicated by the absence (3 L) or reduced (>3 L) desorption of NO and no desorption of N_2O from faceted Ir(210) compared to planar Ir(210), although the amount of N_2 desorption is similar on both surfaces. Table 1 lists the relative integrated areas under the TPD spectra of N-containing products from 40 L of NO adsorbed on faceted and planar Ir(210) at 300 K, normalized to the total integrated areas under the TPD spectra of N-containing products from planar Ir(210). The total TPD peak area of products from faceted Ir(210) is $\sim$75% of that from planar Ir(210), suggesting that a lower saturation coverage of NO is obtained on faceted Ir(210) than that on planar Ir(210) for the same exposure of NO at 300 K. However, the ratio of N_2 peak area to NO peak area is higher from faceted Ir(210) than that from planar Ir(210), and there is no formation of N_2O from faceted Ir(210), implying that faceted Ir(210) is more reactive and selective to N_2 than planar Ir(210) toward NO decomposition. Taken together, these results illustrate structure sensitivity in NO decomposition on planar Ir(210) versus faceted Ir(210).

We also studied the NO decomposition on faceted Ir(210) with different facet sizes (5 and 14 nm). No formation of N_2O is observed from the two faceted surfaces, indicative of no change in selectivity to N_2 for NO decomposition. The TPD spectra of N_2 and NO from the two faceted surfaces appear to be very similar in terms of spectra profile, peak position, and peak intensity (spectra not shown), implying no change in reactivity for NO decomposition either. These results demonstrate that no size effects for NO decomposition over faceted Ir(210), similar to CO oxidation on faceted Ir(210).[12]

3.2. HREELS Study. The HREELS spectra obtained from adsorption of NO on planar Ir(210) at 300 K exhibit only one prominent N$-$O stretching loss feature, ν(N$-$O), at the entire NO exposure range. The ν(N$-$O) peak shifts from 1740 cm^{-1} to 1780 cm^{-1} with increasing NO exposure from 0.2 L to 40 L; the peak position remains the same at $\geq$40 L NO. This N$-$O stretching frequency is assigned to the N$-$O stretching vibration for NO on the atop sites of Ir(210). The assignment is based on detailed comparison with the characteristic N$-$O stretching feature of atop bonded NO on other Ir surfaces[17,18] and other transition metal surfaces[19−27] as summarized in Figure 6, where adsorption of NO on atop sites is not observed for the underlined metal surfaces. The assignment is also supported by our DFT calculations, which will be described in Section 3.3. Figure 7a,b

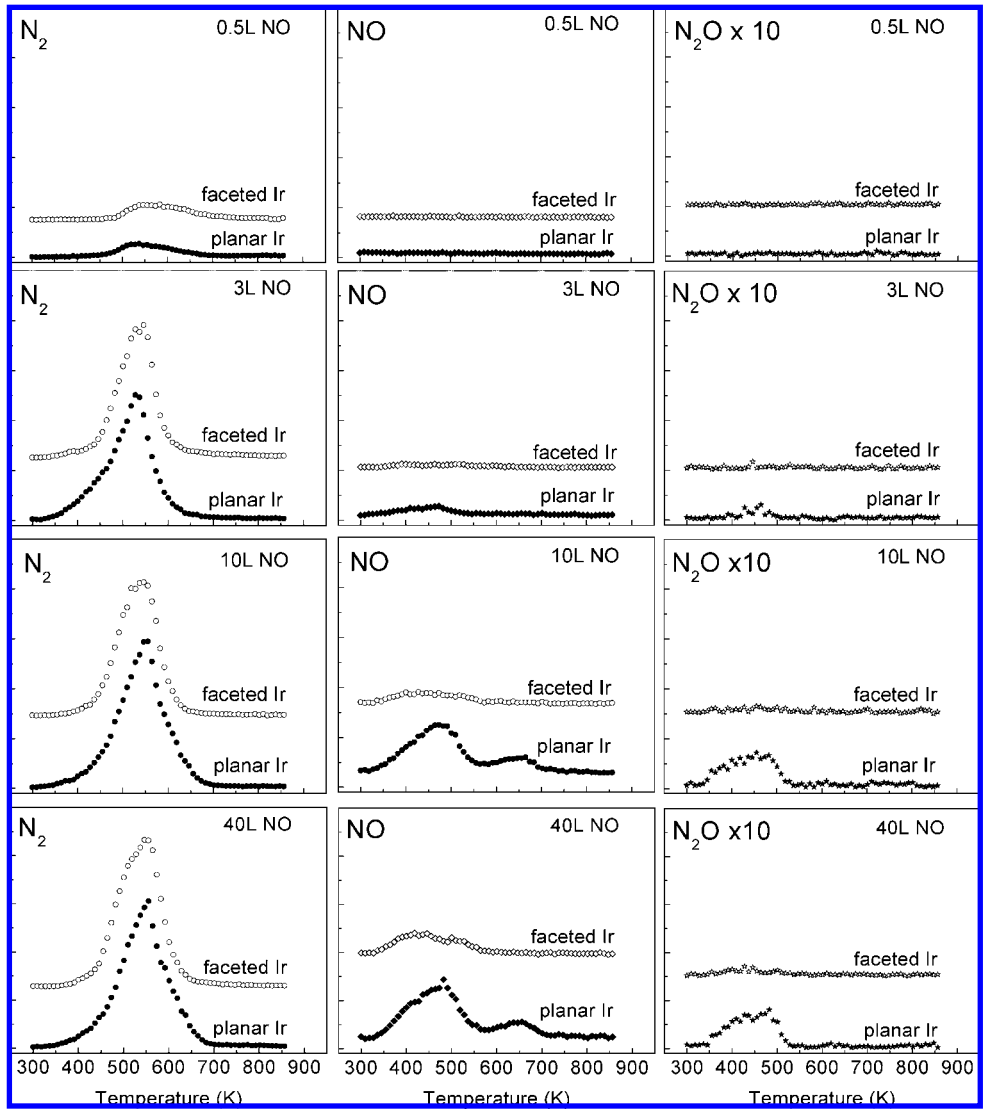

Figure 5. TPD spectra of N_2, NO, and N_2O from adsorption of different exposures of NO at 300 K on faceted and planar Ir(210), respectively.

TABLE 1: Relative TPD Peak Areas of All N-Containing Products for Adsorption of 40 L of NO on Planar and Faceted Ir(210) at 300 K

	N_2	NO	N_2O	NO_2	total
planar Ir(210)	0.65	0.33	0.02	0	1
faceted Ir(210)	0.63	0.11	0	0	0.74

(bottom curve in each case) shows the representative HREEL spectra from adsorption of NO on planar Ir(210) at 300 K.

When NO is adsorbed on faceted Ir(210) at 300 K, the N−O stretching loss feature is dependent on NO exposure: two N−O stretching loss features, ν_1(N−O) and ν_2(N−O), are observed at NO exposure ≤10 L while only one N−O stretching loss feature, ν_2(N−O), is seen at NO exposure > 10 L. The ν_1(N−O) mode increases from 1510 cm^{-1} to 1560 cm^{-1} as NO exposure increases from 0.2 L to 10 L, while the ν_2(N−O) feature increases from 1730 cm^{-1} to 1760 cm^{-1} as NO exposure increases from 0.2 L to 40 L. Figure 7a,b (top curve in each case) shows the representative HREEL spectra from adsorption of NO on faceted Ir(210) at 300 K. The ν_1(N−O) mode is attributed to the charactristic N−O stretching vibration for NO on bridge sites of (110) and {311} faces, while the ν_2(N−O) mode is attributed to the N−O stretching vibration

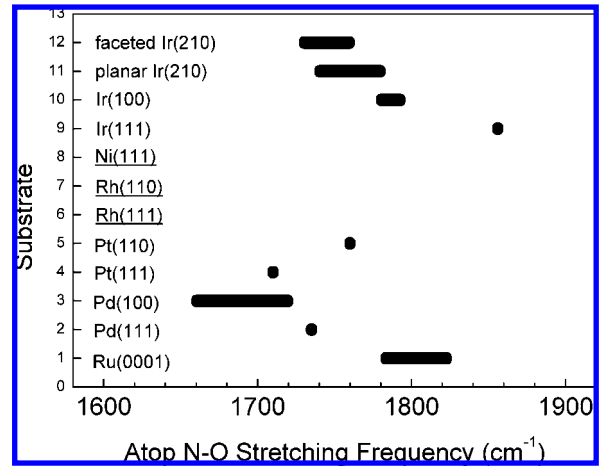

Figure 6. Vibratinal assignments for atop N−O stretching frequency on Ir and other transition metal surfaces.

for NO on atop sites of (110) and {311} faces. The assignments are based on a detailed comparison with the characteristic N−O stretching features of bridge and atop bonded NO on other Ir surfaces[17,18] and other transition metal surfaces[19−27] as summarized in Figures 6 and 8, where adsorption of NO on bridge

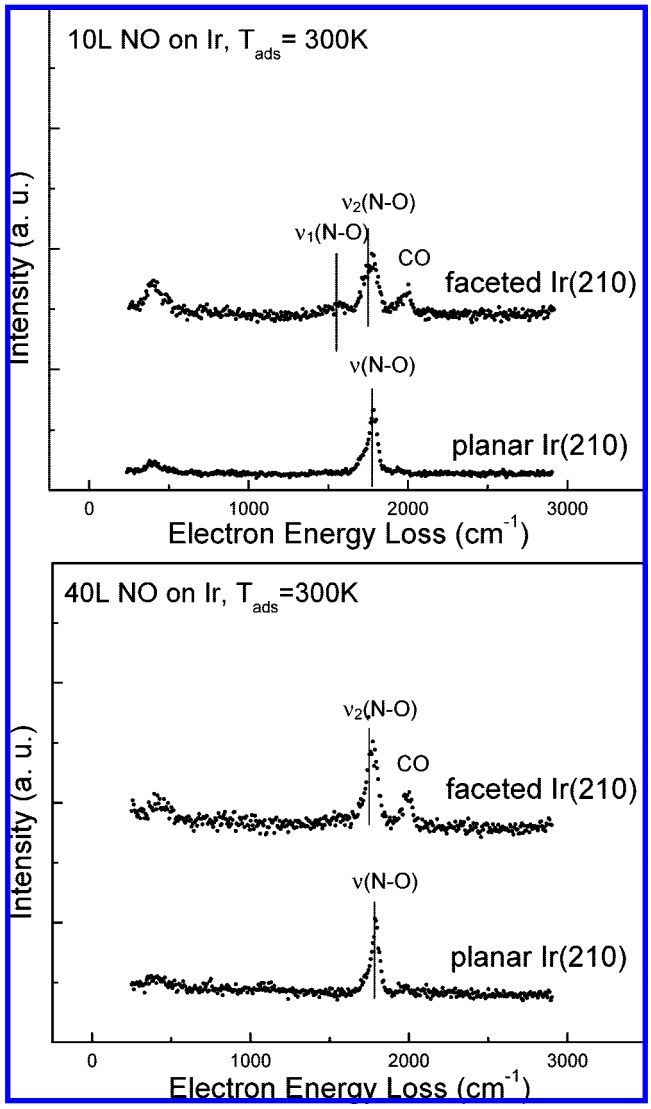

Figure 7. HREELS spectra for adsorption of 10 L (a) and 40 L (b) NO on planar Ir(210) and faceted Ir(210) at 300 K.

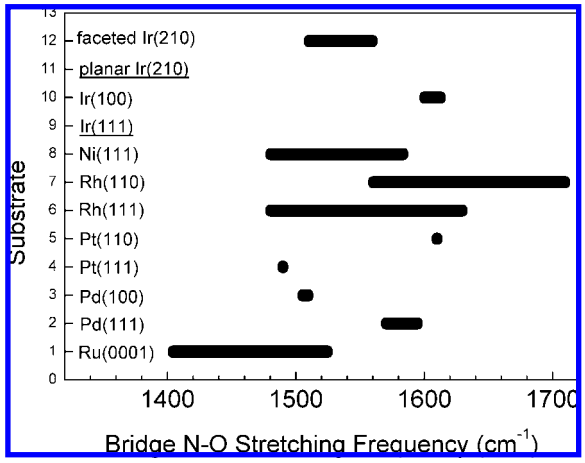

Figure 8. Vibrational assignments for bridge N−O stretching frequency on Ir and other transition metal surfaces.

or atop sites on the underlined metal surfaces is not observed. The assignments are also supported by our DFT calculations, which will be described in Section 3.3, as well as bridging nitrosyl group in organometallic complexes.[28,29] The vibrational feature for CO (~2000 cm^{-1}) is seen in the spectra and is due

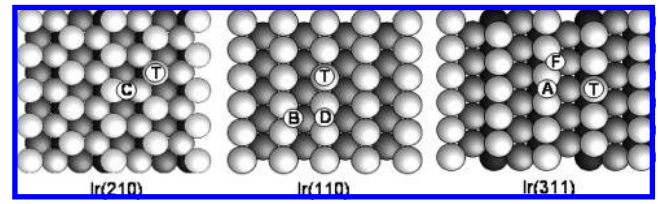

Figure 9. Top view of hard-sphere bulk truncation models of Ir(210), Ir(110), and Ir(311) showing adsorption sites for NO.

to background gas adsorption. The observation that NO molecules adsorb on both bridge and atop sites of faceted Ir(210) at low NO coverage but only on atop sites of planar Ir(210) indicates structure sensitivity in adsorption sites of NO on Ir.

3.3. DFT Study. DFT calculations have been carried out for NO on Ir(210), Ir(110), and Ir(311) to determine the preferred NO binding sites and their vibrational frequencies. The binding sites for which calculations were performed are shown in Figure 9, which were used as initial structures in the calculations. The data presented here are for 1 ML NO on Ir(210), Ir(110), and Ir(311), where 1 ML refers to one geometrical monolayer. On Ir(210), NO is found to bind most strongly on the atop (T) sites with a binding energy (BE) of 2.95 eV, which is 0.53 eV more stable than NO on the bridge (C) sites. This finding supports our HREELS data for NO on planar Ir(210) where only atop bound NO is observed as described in Section 3.2. The calculated N−O stretching frequency for NO on the atop sites of Ir(210) is 1869 cm^{-1}. On Ir(110), NO binds most strongly on the atop (T) and bridge (D) sites with BEs of 2.35 eV and 2.31 eV, respectively. At the hollow (B) sites, NO is not stable and moves to nearby D sites. The calculated N−O stretching frequencies for NO on the atop and bridge sites of Ir(110) are 1793 cm^{-1} and 1665 cm^{-1}, respectively. On Ir(311), NO binds most strongly on bridge (A) and atop (T) sites with BEs of 2.51 eV and 2.34 eV, respectively. At the hollow (F) sites, NO is not stable and moves to nearby A sites. The calculated N−O stretching frequencies for NO on bridge and atop sites of Ir(311) are 1676 cm^{-1} and 1864 cm^{-1}, respectively. Taking DFT data from NO/Ir(110) and NO/Ir(311) together, the calculations support our HREELS data for NO on faceted Ir(210), where both bridge and atop bound NO species are observed at fractional NO coverage. The fact that the calculated BEs for NO on Ir(311) are higher than those for NO on Ir(110) suggests that on faceted Ir(210) NO first adsorbs on {311} and then on (110) faces. Since the differences in BEs between bridge bound NO and atop bound NO on either Ir(110) or Ir(311) are relatively small, the disappearance of bridge bound NO on faceted Ir(210) at saturation coverage is most likely due to the switching of NO from bridge to atop sites to maximize the number of adsorbed NO on the surface.

4. Discussion

When planar and faceted Ir(210) are saturated with 40 L of NO at 300 K, the dominant thermal desorption product is N_2, and the desorption of NO is much less than that of N_2 (the integrated NO area is less than half of the integrated N_2 area on both surfaces); only traces of N_2O are observed from planar Ir(210) whereas no N_2O desorbs from faceted Ir(210), as seen in Figures 2 and 5. These are in sharp contrast to thermal decomposition products from single crystal Pt,[30,31] Rh,[32] and Pd[33] surfaces presaturated by NO at room temperature, where the amount of NO desorption is comparable to or larger than half of that of N_2, and N_2O forms in a large amount (the integrated N_2O area is comparable to or larger than half of the

integrated N_2 area). Therefore, our data demonstrate that both planar and faceted Ir(210) are more active and selective to N_2 formation than Pt, Rh, and Pd in NO decomposition. It is important to point out that Pt, Rh, and Pd are the constituents of commercial three-way catalysts. Using DFT calculations, Liu et al. have compared barriers for dissociation of NO (E_{N-O}) and formation of N_2 (E_{N2}), N_2O (E_{N2O}), and NO_2 (E_{NO2}) on Ir(211) and Pt(211), and they have confirmed that Ir indeed has higher reactivity and selectivity to N_2 in decomposition of NO for the same surface structure of Ir and Pt surfaces.[34] On Ir(211) the barrier for NO dissociation is lower than the barrier for N_2 formation, and the barriers for both NO dissociation and N_2 formation are much lower than the barriers for formation of N_2O and NO_2: $E_{N-O} < E_{N2} \ll E_{N2O} < E_{NO2}$.[34] Therefore, the formation of N_2O and NO_2 is energetically hindered on Ir(211). In contrast, on Pt(211) the barrier for NO dissociation is higher than the barriers for formation of N_2 and N_2O: $E_{N2} < E_{N2O} < E_{N-O} < E_{NO2}$) on Pt(211).[34] This implies that N_2O forms together with N_2 as soon as the N−O bond scission occurs on Pt(211). Therefore, the formation of N_2O is energetically favored on Pt(211) although formation of NO_2 is energetically forbidden. Our experimental data together with Liu et al.'s calculations demonstrate that Ir should be a promising catalyst component to remove NO than Pt.

Thermal decomposition of NO was previously observed on a W surface where an open site was proposed to be involved in the rate-controlling step for NO decomposition.[35] A similar dissociation mechanism may be also involved in the activation step for the decomposition of NO on Ir(210). As described in Section 3, NO adsorbs molecularly on Ir(210) at 300 K and binds to one-site (atop site) of the surface via N atom. Upon heating, NO on a one-site binding configuration may interconvert to a two-site binding configuration via N and O atoms, which is a precursor for the N−O bond breaking at elevated temperature. Once NO undergoes N−O bond scission, most of transient N atoms recombine and desorb as N_2 so that the N−O bond breaking is the rate-controlling step for N_2 desorption from NO decomposition on Ir(210) while remaining transient N atoms react with adsorbed NO to give rise to N_2O that desorbs concomitantly with NO (Figure 2). As shown in Figure 2, NO undergoes complete decomposition on Ir(210) at very low NO exposure ($\leq$1 L), which might be attributed to enough open sites available on Ir(210) at such low coverage for complete interconversion of adsorbed NO from one-site binding to two-site binding prior to dissociation. The complete decomposition of NO on both planar and faceted Ir(210) at 0.5 L of NO (Figure 5) illustrates that adsorption of NO on bridge sites of Ir is not required for Ir to achieve high reactivity in NO decomposition, since NO adsorbs on atop sites of planar Ir(210) but on both bridge and atop sites of faceted Ir(210).

The high reactivity and selectivity to N_2 of planar Ir(210) in NO decomposition might be attributed to the presence of low-coordination C_6 sites on the surface. Whereas the high reactivity and selectivity of faceted Ir(210) in NO decomposition may be associated with the presence of finite areas of facet planes as well as edges, corners, and defects introduced by the formation of the faceted surface. Although (110) and {311} facet planes do not contain the C_6 sites present on planar Ir(210), both contain C_7 sites,[36] and Ir edge and corner atoms at the boundaries of the facet planes also contain C_6 sites which have higher density with smaller facet size. Due to much lower density of edge and corner atoms on faceted Ir(210) than that of C_6 sites on planar Ir(210), as well as absence of size effects in thermal decomposition of NO, C_7 sites on the finite facet planes of (110) and {311} may play the key role in NO decomposition on the faceted surface. The absence of N_2O formation on faceted Ir(210) may be ascribed to the following two facts. First, no formation of N_2O is observed on the Ir(110) and Ir(211) crystal surfaces as reported by other groups.[37,38] Second, Ir(311) or Ir(2(111)×(100)) has similar structure to Ir(211) or Ir(3(111)×(100)) containing (111) terraces and (100) steps but with higher step density on Ir(311), and this stepped structure of Ir is believed to be responsible for high selectivity to N_2 in NO decomposition over Ir(211).[34] The unusual high reactivity of faceted Ir(210) in NO decomposition may benefit from the presence of nanoscale features of faceted Ir(210) since reactivity of the Ir(110) crystal surface in NO decomposition is low (desorption of NO is comparable to that of N_2 from decomposition of NO on Ir(110) crystal surface) as reported previously.[37] Using Monte Carlo simulations, Persson et al. have shown that the reaction kinetics on faceted nanocrystals can be remarkably different from those on single crystal surfaces due to nontrivial coupling of the kinetics of the individual facets.[39]

5. Conclusion

The adsorption and decomposition of NO have been investigated on planar Ir(210) and nanofaceted Ir(210) with facet size ranging from 5 to 14 nm in the temperature range of 300−850 K using TPD, HREELS, and DFT. Both surfaces favor decomposition of NO with high selectivity to N_2. Preadsorbed CO does not inhibit conversion of NO to N_2 on Ir(210), but it improves selectivity to N_2; however, O atoms from self-decomposition of NO deactivates Ir(210) toward NO decomposition. Significant differences in desorption rates of N_2, NO, and N_2O are exhibited between the planar and the faceted surfaces toward NO decomposition, indicative of structure sensitivity in NO decomposition on Ir. NO adsorbs on atop sites of planar Ir(210) but on both bridge and atop sites of faceted Ir(210) at low NO coverage, indicating structure sensitivity in adsorption sites of NO on Ir. No evidence has been found for size effects in thermal decomposition of NO over faceted Ir(210) for average facet size ranging from 5 to 14 nm. The results obtained in this work are relevant to preparation of Ir-based catalysts for controlling NO emission in environmental applications.

Acknowledgment. In memory of Prof. Theodore E. Madey who passed away on July 27, 2008, at the age of 70. The Rutgers University authors acknowledge support from the U.S. Department of Energy, Office of Basic Energy Sciences (Grant DE-FG02-93ER14331). The University of Delaware authors acknowledge support from the U.S. Department of Energy, Office of Basic Energy Sciences (Grant No. DE-FG02-00ER15104). P.K. and T.J. gratefully acknowledge support by the German Academic Exchange Service (DAAD) and the Deutsche Forschungsgemeinschaft (DFG) within the Emmy-Noether-Program.

References and Notes

(1) Parvulescu, V. I.; Grange, P.; Delmon, B. *Catal. Today* **1998**, *46*, 233.
(2) Garin, F. *Appl. Catal., A* **2001**, *222*, 183.
(3) Amiridis, M. D.; Mihut, C.; Maciejewski, M.; Baiker, A. *Top. Catal.* **2004**, *28*, 141.
(4) Burch, R.; Breen, J. P.; Meunier, F. C. *Appl. Catal., B* **2002**, *39*, 283.
(5) Ermanoski, I.; Pelhos, K.; Chen, W.; Quinton, J. S.; Madey, T. E. *Surf. Sci.* **2004**, *549*, 1.
(6) Chen, W.; Ermanoski, I.; Madey, T. E. *J. Am. Chem. Soc.* **2005**, *127*, 5014.

(7) Wang, H.; Chen, W.; Madey, T. E. *Phys. Rev. B* **2006**, *74*, 205426.
(8) Wang, H.; Chan, A. S. Y.; Chen, W.; Kaghazchi, P.; Jacob, T.; Madey, T. E. *ACS Nano* **2007**, *1*, 449.
(9) Wang, H. Ph.D. Thesis, Rutgers University, 2008.
(10) Shen, Q.; Chen, W.; Madey, T. E. Unpublished data.
(11) Chen, W.; Ermanoski, I.; Wu, Q.; Madey, T. E.; Hwu, H. H.; Chen, J. G. *J. Phys. Chem. B* **2003**, *107*, 5231.
(12) Chen, W.; Ermanoski, I.; Jacob, T.; Madey, T. E. *Langmuir* **2006**, *22*, 3166.
(13) Segall, M. D.; Lindan, P. J. D.; Probert, M. J.; Pickard, C. J.; Hasnip, P. J.; Clark, S. J.; Payne, M. C. *J. Phys.: Condens. Matter* **2002**, *14*, 2717.
(14) Vanderbilt, D. *Phys. Rev. B* **1990**, *41*, 7892.
(15) Perdew, J. P.; Burke, K.; Ernzerhof, M. *Phys. Rev. Lett.* **1996**, *77*, 3865.
(16) Monkhorst, H. J.; Pack, J. D. *Phys. Rev. B* **1976**, *13*, 5188.
(17) Fujitani, T.; Nakamura, I.; Kobayashi, Y.; Takahashi, A.; Haneda, M.; Hamada, H. *J. Phys. Chem. B* **2005**, *109*, 17603.
(18) Gardner, P.; Martin, R.; Nalezinski, R.; Lamont, C. L. A.; Weaver, M. J.; Bradshaw, A. M. *J. Chem. Soc., Faraday Trans.* **1995**, *91*, 3575.
(19) Thiel, P. A.; Weinberg, W. H.; Yates, J. T. *J. Chem. Phys.* **1979**, *71*, 1643.
(20) Wickham, D. T.; Banse, B. A.; Koel, B. E. *Surf. Sci.* **1991**, *243*, 83.
(21) Jorgensen, S. W.; Canning, N. D. S.; Madix, R. J. *Surf. Sci.* **1987**, *179*, 322.
(22) Gland, J. L.; Sexton, B. A. *Surf. Sci.* **1980**, *94*, 355.
(23) Gorte, R. J.; Gland, J. L. *Surf. Sci.* **1981**, *102*, 348.
(24) Root, T. W.; Fisher, G. B.; Schmidt, L. D. *J. Chem. Phys.* **1986**, *85*, 4679.
(25) Cautero, G.; Astaldi, C.; Rudolf, P.; Kiskinova, M.; Rosei, R. *Surf. Sci.* **1991**, *258*, 44.
(26) Chen, J. G.; Erley, W.; Ibach, H. *Surf. Sci.* **1989**, *224*, 215.
(27) Chen, J. G.; Erley, W.; Ibach, H. *Surf. Sci.* **1990**, *227*, 79.
(28) Ghedini, M.; Neve, F. *J. Chem. Soc., Dalton Trans.* **1984**, 1417.
(29) Johnson, B. F. G.; Raithby, P. R.; Zuccaro, C. *J. Chem. Soc., Dalton Trans.* **1980**, 99.
(30) Mukerji, R. J.; Bolina, A. S.; Brown, W. A. *Surf. Sci.* **2003**, *547*, 27.
(31) Jiang, Z.; Huang, W.; Tan, D.; Zhai, R.; Bao, X. *Surf. Sci.* **2006**, *600*, 4860.
(32) Castner, D. G.; Somorjai, G. A. *Surf. Sci.* **1979**, *83*, 60.
(33) Hirsimäki, M.; Suhonen, S.; Pere, J.; Valden, M.; Pessa, M. *Surf. Sci.* **1998**, *402*−*404*, 187.
(34) Liu, Z.-P.; Jenkins, S. J.; King, D. A. *J. Am. Chem. Soc.* **2003**, *125*, 14660.
(35) Yates, J. T.; Madey, T. E. *J. Chem. Phys.* **1966**, *45*, 1623.
(36) Nicholas, J. F. *An atlas of models of crystal surfaces*; Gordon and Breach: New York, 1965.
(37) Ibbotson, D. E.; Wittrig, T. S.; Weinberg, W. H. *Surf. Sci.* **1981**, *110*, 294.
(38) Nakamura, I.; Suzuki, K.; Takahashi, A.; Haneda, M.; Hamada, H.; Fujitani, T. *J. Vac. Sci. Technol. A* **2007**, *25*, 1143.
(39) Persson, H.; Thormählen, P. *J. Vac. Sci. Technol. A* **1999**, *17*, 1721.

JP808143P